Vol 11 No 9, September 2002
1009-1963/2002/11(09)/0869-07

Chinese Physics

© 2002 Chin. Phys. Soc.
and IOP Publishing Ltd

Gas flow characteristics in straight silicon microchannels*

Ding Ying-Tao(丁英涛), Yao Zhao-Hui(姚朝晖)†, and Shen Meng-Yu(沈孟育)

Department of Engineering Mechanics, Tsinghua University, Beijing 100084, *China*

(Received 21 March 2002; revised manuscript received 27 May 2002)

Experiments have been conducted to investigate nitrogen gas flow characteristics through four trapezoidal silicon microchannels with different hydraulic diameters. The volume flow rate and pressure ratio are measured in the experiments. It is found that the friction coefficient is no longer a constant, which is different from the conventional theory. The characteristics are first explained by the theoretical analysis. A simplified rectangular model (rectangular straight channel model) is then proposed. The experimental results are compared with the theoretical predictions based on the simplified rectangular model and the two-dimensional flow between the parallel-plate model which was usually used. The difference between the experimental data and the theoretical predictions is found in the high-pressure ratio cases. The influence of the gas compressibility effect based on the Boltzmann gas kinetic analysis method is studied to interpret the discrepancy. We discuss two important factors affecting the application extent of different prediction models.

Keywords: gas flow, friction coefficient, rectangular model, compressibility
PACC: 0340, 0710C, 4760

1. Introduction

In microelectromechanical systems (MEMS), especially in micro-fluidic systems consisting of micropumps and microvalves, the microchannel is one of the essential components. The trapezoidal microchannel is a kind widely used microchannels.[1] Studying the flow characteristics in different microchannels is important for designing and optimizing MEMS components, so it has more and more become the focus of study. The hydraulic diameter of microchannels ranges from 1 μm to 1000 μm. There are some different characteristics between microflow and macroflow, such as the gas flow in microchannels which have a low Reynolds number while concurrently maintaining a high subsonic Mach number.

Wu *et al*[2] measured the gas flow frictional characteristics of microchannels etched on silicon wafers. The cross section of the microchannels was trapezoidal with the width ranging from 130 μm to 200 μm. In their study, nitrogen, hydrogen and argon gases were used and the theoretical predictions were based on the circular axisymmetrical flow theory. It was observed that the measured friction factors were higher than the theoretical predictions.

Harley *et al*[3] presented experimental results and theoretical investigations of the compressible gas flow with low Reynolds number and high subsonic Mach number in microchannels etched on silicon wafers. The microchannels had a width of 100 μm, a length of 10^4 μm and a depth of 0.5–20 μm. The cross section was trapezoidal. In their study, nitrogen, helium and argon gases were used and theoretical predictions were obtained by solving numerically the two-dimensional (2D) Navier–Stokes equations and energy equation for the compressible flow of gas between two isothermal parallel plates. The measured friction factors were in accordance with the theoretical predictions.

Arkilic *et al*[4] studied gaseous slip flow in long microchannels. The microchannel had a width of 52.25 μm, a depth of 1.33 μm and a length of 7500 μm with the pressure ratio ranging from 1.6 to 4.2; the cross section was trapezoidal. Helium gas was used as a working fluid. The numerical results were obtained by solving the 2D perturbation expansion of the Navier–Stokes equations with a first-order wall-velocity slip flow between two isothermal parallel plates. The measured relationships between mass flow and pressure ratio were in agreement with the theoretical prediction of first-order velocity slip but deviated from that of no-slip. These discrepancies were attributed to the rarefied gas effects.

*Project supported by the Foundation of the Ministry of Education of China for Returned Scholars, the Foundation of the Chinese "985" Project, and the Foundation of the Tsinghua Micro/Nano Technical Center.

†Author to whom correspondence should be addressed. E-mail: yaozh@tsinghua.edu.cn

In this paper, our objectives are to experimentally investigate the gas flow characteristics of trapezoidal microchannels etched on silicon wafers, to study the flow friction characteristics and to attempt to propose an adaptive theoretical prediction model for a specified microchannel.

2. Fabrication

The fabrication process included bulk-silicon etching and silicon–glass electrostatic bonding. A 350 μm thick (100) double-sided polished silicon wafer was covered at the front side by a 300 nm thick silicon dioxide, followed by low-pressure chemical vapour deposition (LPCVD) of 200–250 nm of silicon nitride. Next, the microchannel was etched on silicon nitride. The front side of silicon wafer was etched by the potassium hydroxide wet method. Anisotropic etching was used to form the inlet/outlet holes from the back side of the wafer. The holes were approximately $2\times2\text{mm}^2$ in area and 330 μm in depth. Finally, the sample was anodically bonded to the Pyrex glass to seal it. A brass holder with stainless-steel tubes was glued to the back side of the silicon wafer to ensure stable connections between the inlet/outlet chambers and the stainless-steel tubes.

Precise measurements of the dimensions of a microchannel are important for studying the flow characteristics in microchannels. In the experiments, the width of the microchannels was measured with a calibrated scanning electron microscope (Model CSM-950). The depth of the microchannels was measured optically with a calibrated microscope reticle at 400× or with a surface profilometer. The roughness of the microchannels was measured with a laser surface interferometric microscope (Model WYKO), showing a roughness of about 2%.

The dimensions of four different microchannels are listed in Table 1. A photograph of the silicon microchannel, taken with the laser surface interferometric microscope, is shown in Fig.1. The trapezoidal cross section of the silicon microchannel is shown in Fig.2.

Table 1. Dimensions of the trapezoidal silicon microchannels.

No	Length /mm	Width /μm	Depth /μm	Hydraulic diameter /μm
1	11.5	60	20	26
2	40.5	100	20	31.1
3	40.5	250	20	36.2
4	40.5	1000	20	39

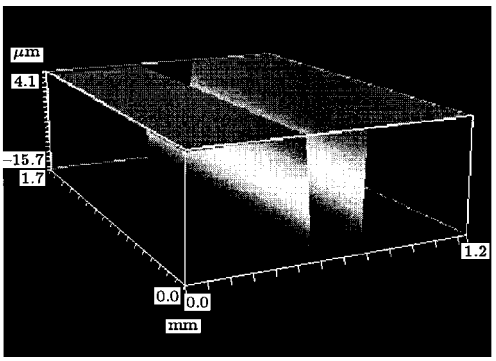


Fig.1. A photograph of the silicon microchannel, taken with the laser surface interferometric microscope.

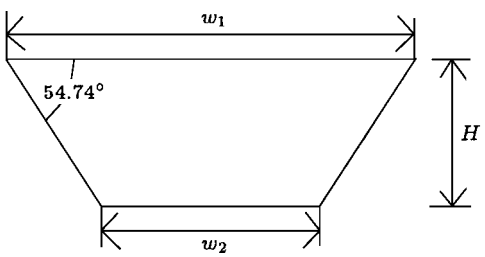


Fig.2. Trapezoidal cross section of the silicon microchannel.

3. Experimental apparatus and procedures

The apparatus used for the experiments is shown in Fig.3. The experimental apparatus consists of: a high-pressure cylinder whose outlet is connected to two pressure regulators; a 0.3 μm fine filter which is used to prevent the microchannel from being clogged by other materials; a constant pressure tank on which a pressure sensor and a temperature sensor are connected; a test section; and a volume flow monitor.

In the experiment, gas flows from a regulated high-pressure cylinder, through a fine filter, a constant pressure tank, the test section, and finally into the flow monitor apparatus. During a run of the measurement, by regulating the pressure in the tank, different volume flow rates are obtained. Some groups of pressure–volume flow rate curves are obtained as well. The volume flow rate is obtained by measuring the time for exhausting the volume of liquid injected into a measuring tube.

In each measurement, when the pressure is adjusted to the desired value by the pressure regulator, to ensure the accuracy of the test, the value has to be stable for 10 min. At the same time, the flow rate is considered to reach a steady state when the pressure

value no longer changes. The value of the volume flow rate is measured three times under the same pressure.

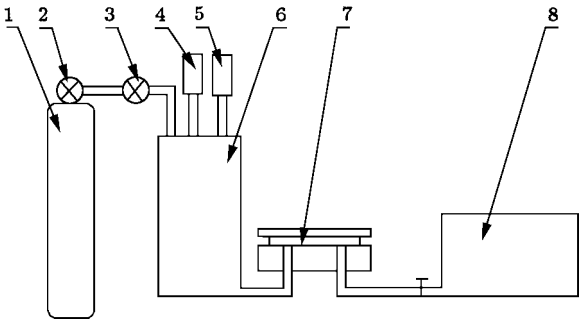


Fig.3. Schematic diagram of the experimental apparatus: 1, high-pressure gas cylinder; 2, pressure regulator; 3, pressure regulator with fine filter; 4, pressure sensor; 5, temperature sensor; 6, stagnant chamber; 7, microchannel test section; 8, flow monitor apparatus.

4. Analytical model

In this work, the Knudsen numbers of the microchannels were measured in the range from 0.000204 to 0.00245, thus the flow characteristics are thought to be in the continuum flow field according to Ref.[5]. Theoretical predictions are made based on solving the Navier–Stokes equations and mass conservation equation to obtain the analytical expressions of velocity distributions. After this, the relationships between mass flow rate and inlet/outlet pressure ratio are obtained by integrating the mass flow rate in the streamwise direction, assuming that the gas satisfies the perfect gas state equation. Thus the gas compressibility effect could be partly considered in the theoretical predictions. When the order of magnitude of the width is close to that of the depth in a microchannel, large errors would be induced if the prediction were based on the 2D flow between the parallel-plate model[4]. We then propose a simplified rectangular model in which the trapezoidal shape is approximated by the rectangular. In the following, two different theoretical predictions are compared with the experimental results. From the comparison, we see that the depth-to-width ratio and the pressure ratio have significant influence on the selection of the models to be used in predictions.

4.1. Some relative parameters

In the experiments, only the volume flow rate Q_{v} and the inlet/outlet pressure difference ΔP are measured. Other parameters, such as Reynolds number Re, Knudsen number Kn, friction factor f and friction coefficient C_{f}, can be obtained by the following formulae:

Reynolds number

$$Re = \frac{D_{\mathrm{h}} Q_{\mathrm{v}}}{A\nu}, \tag{1}$$

where D_{h} is the hydraulic diameter, A is the area of the cross section, ν is the kinematical viscosity of the fluid and Q_{v} is the volume flow rate;

Knudsen number

$$Kn = \frac{\lambda}{D_{\mathrm{h}}}, \tag{2}$$

where λ is the molecule mean free path;

Friction factor and average velocity

$$f = \frac{\Delta P}{L} \frac{2D_{\mathrm{h}}}{\rho u_{\mathrm{av}}^2}, \tag{3}$$

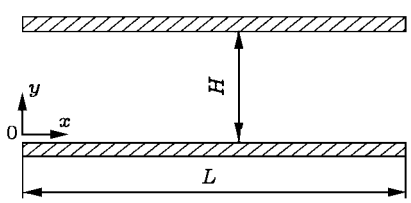
where $u_{\mathrm{av}} = \dfrac{Q_{\mathrm{v}}}{A}$;

Friction coefficient

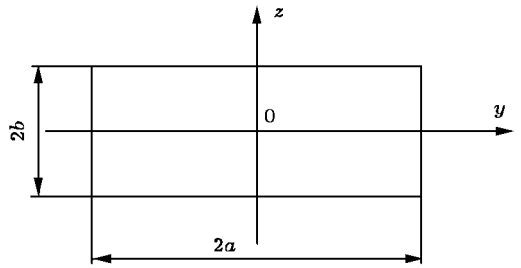
$$C_{\mathrm{f}} = f \cdot Re. \tag{4}$$

4.2. 2D flow model between parallel plates

Referring to Fig.4(a), based on the Poiseuille flow laminar theory, by solving the incompressible 2D Navier–Stokes equations under the no-slip boundary conditions on solid walls, the velocity profile function in the flow field between the two parallel plates is expressed as follows[6]



(a) parallel plates model



(b) rectangular model

Fig.4. Cross section of the microchannel.

$$u(y) = \frac{H^2}{2\mu}\frac{\mathrm{d}P}{\mathrm{d}x}\left(\frac{y^2}{H^2} - \frac{y}{H}\right), \tag{5}$$

where H is the depth of the microchannels (see Fig.2).

Assuming that the gas satisfies the perfect gas state equation, we obtain

$$\rho(x) = \frac{P(x)}{RT}. \tag{6}$$

The mass flow rate is calculated from $\int \rho u(y)\mathrm{d}y = c$. The relationship between the mass flow rate and the pressure ratio can be obtained by integrating the mass flow rate in the streamwise direction.

$$\dot{m} = \frac{H^3 w_1 P_{\mathrm{out}}^2}{24\mu LRT}(\pi^2 - 1), \tag{7}$$

where $\pi = P_{\mathrm{in}}/P_{\mathrm{out}}$ is the inlet/outlet pressure ratio, w_1 is the width of the microchannels (Fig.2), and L is the length of the microchannels.

4.3. Rectangular flow model

Referring to Fig.4(b), the velocity profile for rectangular ducts has been determined using an analogy with the stress function of the theory of elasticity[7] by Dryden *et al*[8] and Marco and Han.[9] The velocity profile, provided by the solution of the incompressible Navier–Stokes equations under the no-slip boundary condition, is expressed as

$$u = \frac{1}{2\mu}\left(-\frac{\mathrm{d}P}{\mathrm{d}x}\right)\left[b^2 - z^2 + \frac{32b^2}{\pi^3} \times \sum_{n=0}^{\infty} \frac{(-1)^n \mathrm{ch}\left(\frac{2n+1}{2b}\pi y\right)\cos\left(\frac{2n+1}{2b}\pi z\right)}{(2n+1)^5 \mathrm{ch}\left(\frac{2n+1}{2b}\pi a\right)}\right], \tag{8}$$

with $a = (w_1 + w_2)/4$, $b = H/2$.

Assuming that the gas satisfies the perfect gas state equation, through integrating the mass flow rate in the streamwise direction, we obtain the relationship between mass flow rate and pressure ratio

$$\dot{m} = \frac{ba^3 P_{\mathrm{out}}^2}{8\mu LRT}\left[\frac{16}{3} - \frac{1024a}{\pi^5 b} \times \left(\sum_{n=1,3,5,\cdots}^{\infty} \frac{1}{n^5}\mathrm{th}\frac{\pi bn}{2a}\right)\right](\pi^2 - 1), \tag{9}$$

where $\pi = P_{\mathrm{in}}/P_{\mathrm{out}}$ is the inlet/outlet pressure ratio.

5. Experimental results and analysis

5.1. Pressure ratio and flow rate characteristics

The pressure ratio and flow rate characteristics in the four different microchannels are measured. The inlet/outlet pressure ratio ranges from 2 to 8. The relationship between mass flow rate and the inlet/outlet pressure ratio predicted by formulae (7) and (9) are compared with experimental data. The comparison curves are plotted in Fig.5. It is seen that the depth-to-width ratio and the pressure ratio are two important factors affecting the accuracy of the analytical models.

Concerning the influence of the depth-to-width ratio, when it is higher than 0.08 (see Figs.5(a) and 5(b)), the results obtained using the rectangular model are better than those of the parallel-plate model. When the ratio is equal to 0.08 (Fig.5(c)), the results based on the rectangular model are nearly the same as those of the parallel-plate model. When it is lower than 0.08 (Fig.5(d)), the results of the parallel-plate model are better than those of the rectangular model.

Concerning the influence of the pressure ratio, if the 5% error is regarded as a standard for evaluating the application range of a model, then we can make conclusions as follows. In the range of the pressure ratio lower than 5 (Figs. 5(a) and 5(b)), the analytical predictions made through the rectangular model are very consistent with the experimental results. In the range of the pressure ratio lower than 5 (Fig.5(d)), the analytical predictions of the parallel-plate model are very consistent with the experimental results.

For higher pressure ratios, the predictions of mass flow rate are higher than the experimental data. The discrepancy is attributed to the gas compressibility effect. With increasing pressure ratio, the gas compressibility effect increases, which will be discussed in section 5.3.

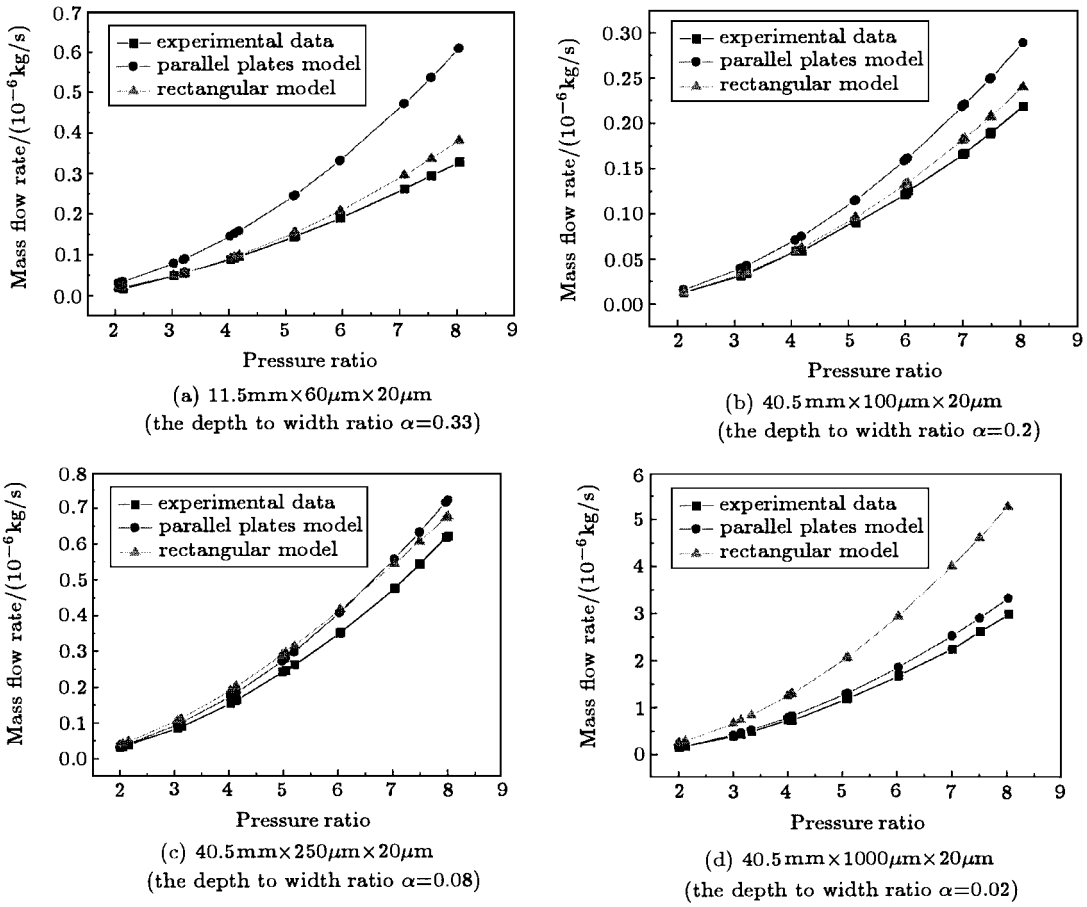


Fig.5. A comparison of the measured data of mass flow rate versus pressure ratio, with the predictions based on the parallel-plate model and the rectangular model.

5.2. Friction characteristics

The friction coefficient C_{f} is an indispensable parameter for describing the flow friction in channels. According to the conventional incompressible laminar flow theory, C_{f} for a trapezoidal channel is a constant as the Reynolds number increases, depending only on the geometry of the cross section[10,11]. In this paper, the experimental data C_{f} is no longer a constant and the characteristics are explained first by theoretical analysis. This is plotted in Fig.6. We conclude that the discrepancy is due to the gas compressibility effect. Because the density in the streamwise direction is not a constant, the relationship between the pressure ratio and the flow rate is not linear. The detailed analysis can be described below. Based on Eqs.(1), (3) and (4), the required relations can be obtained as follows

$$C_{\mathrm{f}} = \frac{2\Delta P D_{\mathrm{h}}^2 A}{\mu L Q_{\mathrm{v}}} = k_1 \frac{\Delta P}{L}\frac{1}{Q_{\mathrm{v}}}, \tag{10}$$

where $k_1 = \dfrac{2D_{\mathrm{h}}^2 A}{\mu}$.

The corresponding mass flow rate is computed by using

$$\begin{aligned} \dot{m}L &= \int_0^L \dot{m}\mathrm{d}x = \int_0^L \rho Q_{\mathrm{v}}\mathrm{d}x \\ &= \int_0^L \frac{P(x)}{RT} k_2 \left(-\frac{\mathrm{d}P}{\mathrm{d}x}\right)\mathrm{d}x \\ &= \frac{k_2}{2RT}(P_{\mathrm{in}}^2 - P_{\mathrm{out}}^2), \end{aligned} \tag{11}$$

where

$$k_2 = \begin{cases} \dfrac{H^3 w_1}{12\mu} & \text{(2D parallel plates model)}, \\ \dfrac{ba^3}{4\mu}\left[\dfrac{16}{3} - \dfrac{1024a}{\pi^5 b}\left(\displaystyle\sum_{n=1,3,5,\cdots}^{\infty} \frac{1}{n^5}\mathrm{th}\frac{\pi b n}{2a}\right)\right] & \text{(rectangular model)}, \end{cases}$$

$$Q_{\rm v} = \frac{\dot{m}}{\rho_{\rm out}} = \frac{\dot{m}}{\frac{P_{\rm out}}{RT}}. \tag{12}$$

Combining Eqs.(10)–(12), $C_{\rm f}$ can be obtained

$$C_{\rm f} = k_3 \frac{P_{\rm out}}{P_{\rm in} + P_{\rm out}}, \tag{13}$$

where

$$k_3 = \begin{cases} \dfrac{48 D_{\rm h}^2 A}{H^3 w_1} & \text{(2D parallel plates model)}, \\ \dfrac{16 D_{\rm h}^2 A}{ba^3 \left[\dfrac{16}{3} - \dfrac{1024a}{\pi^5 b} \left(\displaystyle\sum_{n=1,3,5,\cdots}^{\infty} \dfrac{1}{n^5} \mathrm{th} \dfrac{\pi b n}{2a} \right) \right]} & \text{(rectangular model)}. \end{cases}$$

From Eq.(13), it can be seen that $C_{\rm f}$ is directly proportional to the value $\dfrac{P_{\rm out}}{P_{\rm in} + P_{\rm out}}$. In the experiment, because the outlet pressure $P_{\rm out}$ is constant, the value $\dfrac{P_{\rm out}}{P_{\rm in} + P_{\rm out}}$ decreases with increasing inlet pressure $P_{\rm in}$.

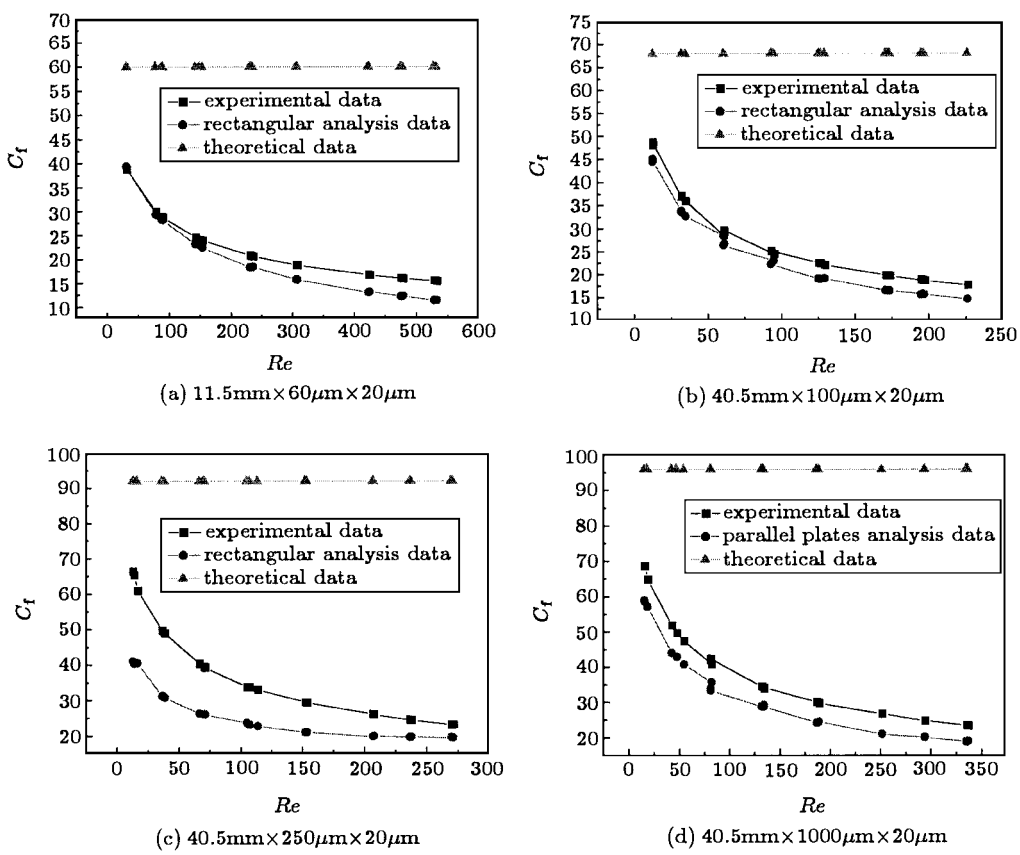


Fig.6. A comparison of the measured data of the friction coefficient $C_{\rm f}$ versus Reynolds number Re, with the value based on the conventional incompressible laminar flow theory and the predicted values based on the rectangular and parallel-plate models.

5.3. Compressibility effects

It is seen in section 5.1 that the experimental data gradually deviate from the theoretical predictions as the pressure ratio increases. The discrepancy between the experimental data and theoretical predictions is attributed to the gas compressibility effect. A simulation for circular axisymmetrical flow based on a Boltzmann gas kinetic analysis method[12] is plotted in Fig.7. As can be seen from Fig.7, the velocity pro-

file gradually deviates from the parabolic distribution with increasing pressure ratio.

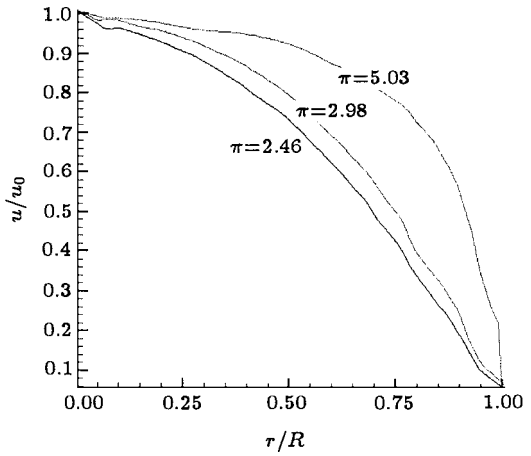


Fig.7. Velocity profile calculated using the Boltzmann gas kinetic analysis method.

6. Conclusions

Experimental investigations and theoretical predictions of nitrogen gas compressible flow in trapezoidal microchannels have been conducted. The experimental results are compared with the theoretical predictions based on a 2D flow between a parallel-plate model and a simplified rectangular flow model. The comparison indicates that two important factors, i.e. the depth-to-width ratio α and the pressure ratio π, affect the application range of different prediction models. When α is higher than 0.08 and π is lower than 5, the rectangular model is recommended; when α is lower than 0.08 and π is lower than 5, the parallel-plate model is recommended; when α is equal to 0.08 and π is lower than 5, either the rectangular model or the parallel-plate model is equally recommended. The experimental data are slightly lower than the theoretical predictions in the high-pressure ratio cases.

Furthermore, the relationships between friction coefficient and Reynolds number have also been studied. It is found that the friction coefficient for a given microchannel is no longer a constant; it varies with Reynolds number. This characteristic is explained first by the theoretical analysis.

These discrepancies can be due mainly to the gas compressibility effect. With increasing pressure ratio, the gas compressibility effect increases and the velocity profile deviates from parabolic distribution gradually. The deviation from the parabolic velocity distribution is qualitatively verified by the simulation results based on the Boltzmann gas kinetic analysis method.

Acknowledgments

The first author gratefully acknowledges the discussions with Professor Wang Xue-Fang and Professor Xu Hong-Qing in Tsinghua University. The authors wish to thank Dr Bottoni Maulizio for reviewing this paper carefully and Tsinghua University Microelectron Center, Tsinghua University Friction Laboratory and Peking University Microelectron Center for supporting the work.

References

[1] Yao Z H *et al* 2002 *Chin. Phys.* **11** 226
[2] Wu P Y and Little W A 1983 *Joule-Thomson Refrigerators Cryogenics* **23** 273
[3] Harley J C *et al* 1995 *J. Fluid Mech.* **284** 257
[4] Arkilic E B *et al* 1997 *J. Microelectromech. Syst.* **6** 167
[5] Janson S W, Helvajian H and Breuer K The American Institute of Aeronautics and Astronautics 99–3802
[6] Rohsenow W M and Choi H Y 1961 *Heat Mass and Momentum Transfer* (New Jersey: Academic)
[7] Timoshenko S P and Goodier J N 1970 *Theory of Elasticity* (New York: Academic)
[8] Dryden H L, Murnaghan F D and Bateman H 1932 *Bull* **84** 197
[9] Marco S M and Han L S 1955 *Trans. Am. Soc. Mech. Eng.* **77** 625
[10] Choi S B, Barrori R G and Warrington R W 1991 *Am. Soc. Mech. Eng. Dynamics Syst. Control Division* **32** 123
[11] Shah R K and London A L 1978 *Laminar Flow Forced Convection in Ducts* (New York: Academic)
[12] Sun X M, Yao Z H and Yang J L 2002 *Acta Phys. Sin.* **51** 1942 (in Chinese)